

Study on Electromagnetic Vibration of Magnetic Gear

Noboru Niguchi, Katsuhiro Hirata

Dept. of Adaptive Machine Systems, Graduate School of Engineering, Osaka
University

2-1, Yamadaoka, Suita, Osaka 565-0871, Japan

E-mail:noboru.niguchi@ams.eng.osaka-u.ac.jp

Abstract :

Magnetic gears have some advantages such as maintenance-free operation and self-overload protection that are not observed in mechanical gears. They were not in practical use due to the low transmission-torque density. But, recently, the practical transmission-torque density could be obtained by developing a magnetic harmonic gear (MHG) operating with harmonic magnetic flux.

We have developed the cogging torque reduction method of MHG to reduce the vibration caused by the cogging torque. But, few studies regarding electromagnetic vibration have not been seen.

This paper describes the electromagnetic vibration of a MHG by employing the coupled analysis between magnetic field and structure, and the results are verified by carrying out measurements by a prototype.

JMAG Users Conference 2010



Study on Electromagnetic Vibration of Magnetic Gear

Noboru Niguchi and Katsuhiro Hirata
 Dept. of Adaptive Machine Systems, Graduate School of Eng.
 Osaka University

Introduction of Hirata-Lab.



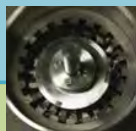
Primary research

Rotation motion

- Magnetic coupling
- Magnetic impact
- Synchronous motors for automobiles



- Magnetic gears



Linear motion

- Actuators for androids
- ACM (Active Control Engine Mount)
- Non-contact linear position sensors

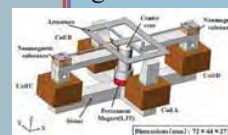


Multi-degree-of-freedom systems

- Spherical actuator



- Resonant optical scanner with 2 degrees-of-freedom



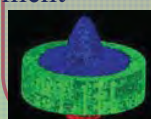
Resonant systems

- Resonant actuator with 2 degrees-of-freedom
- Linear vibration actuators
- Giant magnetostrictive speakers



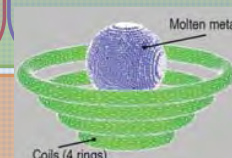
Analysis code development

- Ferrofluid actuators



Ferrofluid

- Electrostatic atomization device
- Electromagnetic levitation of molten metal



Contents

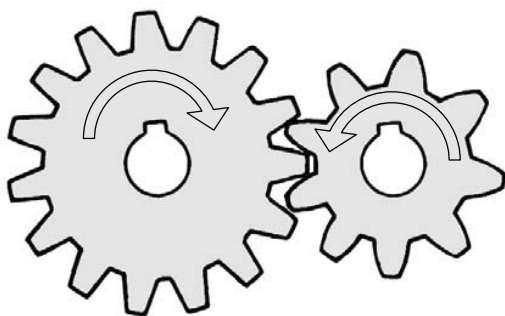


1. Development Background of Magnetic Gears
2. Operating Principles of Magnetic Harmonic Gears
3. Causes of Vibration
 - 3.1. Vibration due to Cogging Torque
 - 3.2. Vibrations due to Electromagnetic Deformation
4. Verification by Measuring Noises
5. Conclusion

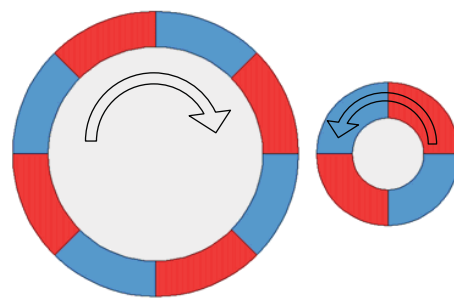
1. Development Background of Magnetic Gears



What is a Magnetic Gear?



Mechanical gear



Magnetic gear

Advantages

- No wear because of no contact
⇒ Maintenance-free operation
- Automatic slip under overload condition
⇒ Protection of equipment

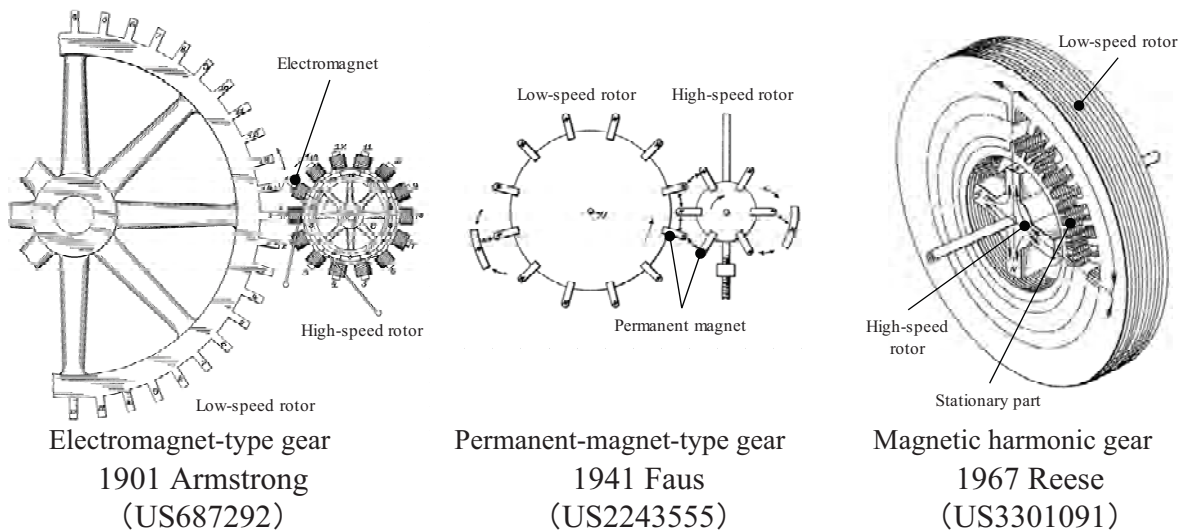
Applications

- Carrier equipment for clean rooms
- Equipment used in space
- Joint of a humanoid robot

1. Development Background of Magnetic Gears



History of Magnetic Gears

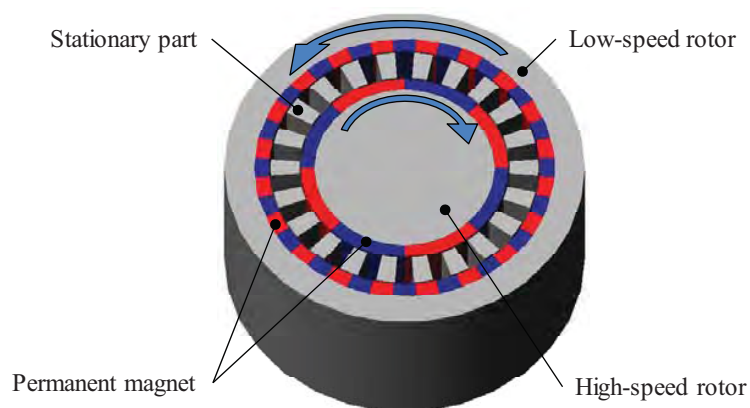


These gears didn't attract attentions
because the transmission torque for a practical use couldn't be obtained.

1. Development Background of Magnetic Gears



Magnetic Harmonic Gear



Surface-Permanent-Magnet-Type Magnetic Harmonic Gear
(SPM-Type Magnetic Harmonic Gear)

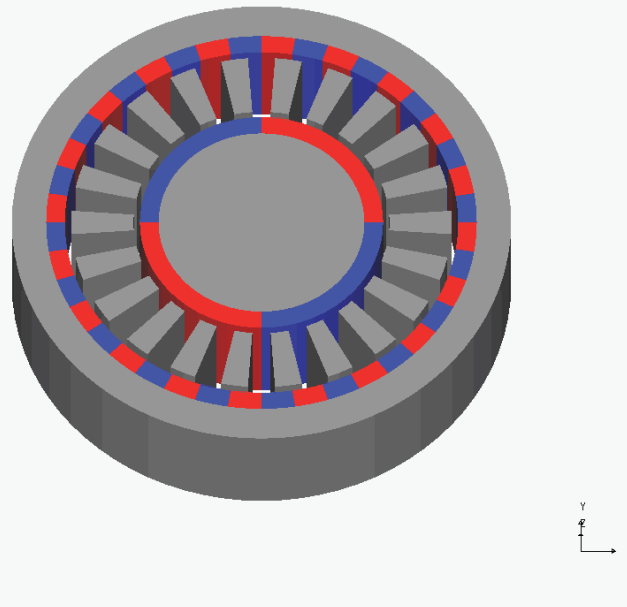
- A high- and low-speed rotor sandwich a stationary part.
- The low-speed rotor rotates by synchronizing to the harmonics generated around the stationary part by the magnetomotive force of the high-speed rotor and permeance of the stationary part.

1. Development Background of Magnetic Gears



Operation of a harmonic type magnetic gear

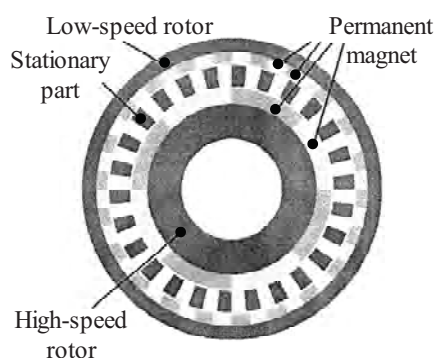
Gear ratio 10: 1



1. Development Background of Magnetic Gears

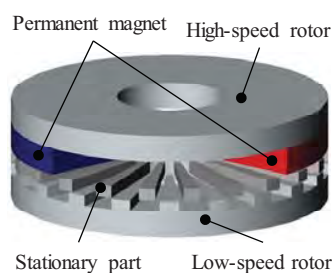


Recent Trends in Magnetic Harmonic Gears



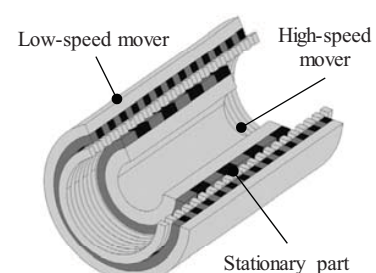
Radial gap type

2001 Atallah and others
(*IEEE Trans. Magn.*)



Axial gap type

2006 Mezani and others
(*J. Appl. Phys.*)



Linear type

2006 Atallah and others
(*IEEJ Trans. IA*)

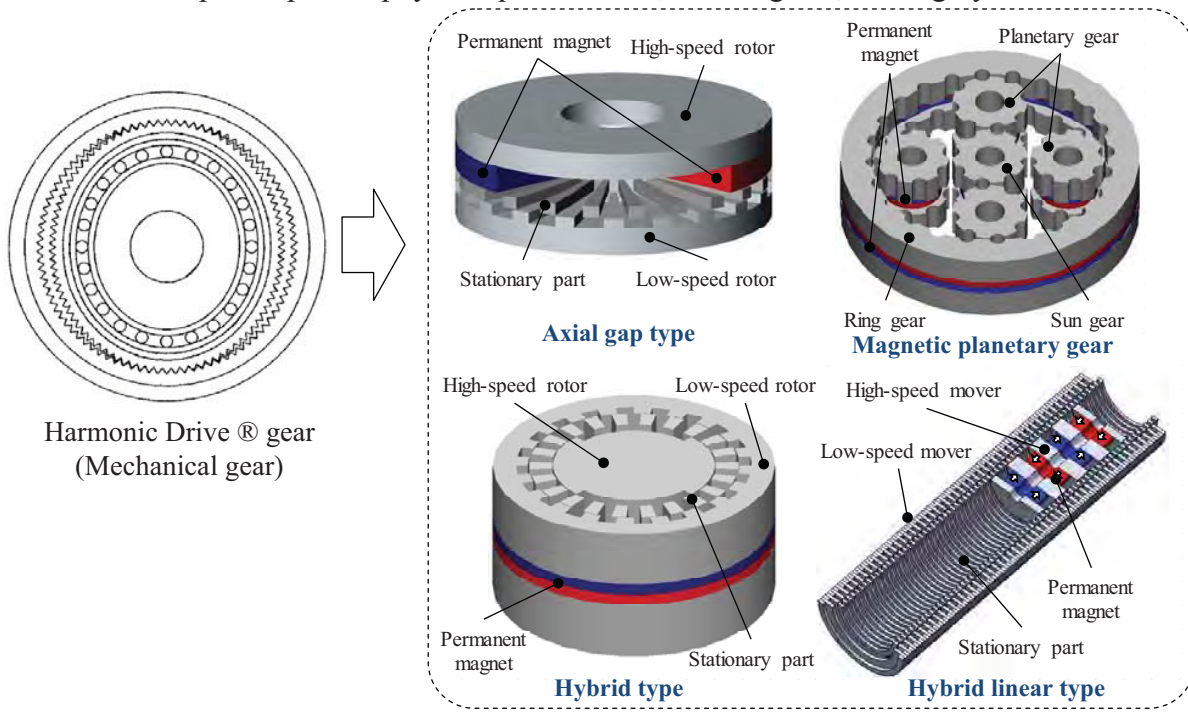
- Magnetic gear research shifted after the report by Atallah and others in 2001.
- Disadvantages in productivity and cost were caused by the large number of magnets required for multipole structures.

1. Development Background of Magnetic Gears



Efforts for Magnetic Gears at the Hirata Laboratory, Osaka University

■ Development philosophy: Simple structure, few magnets, and highly robust

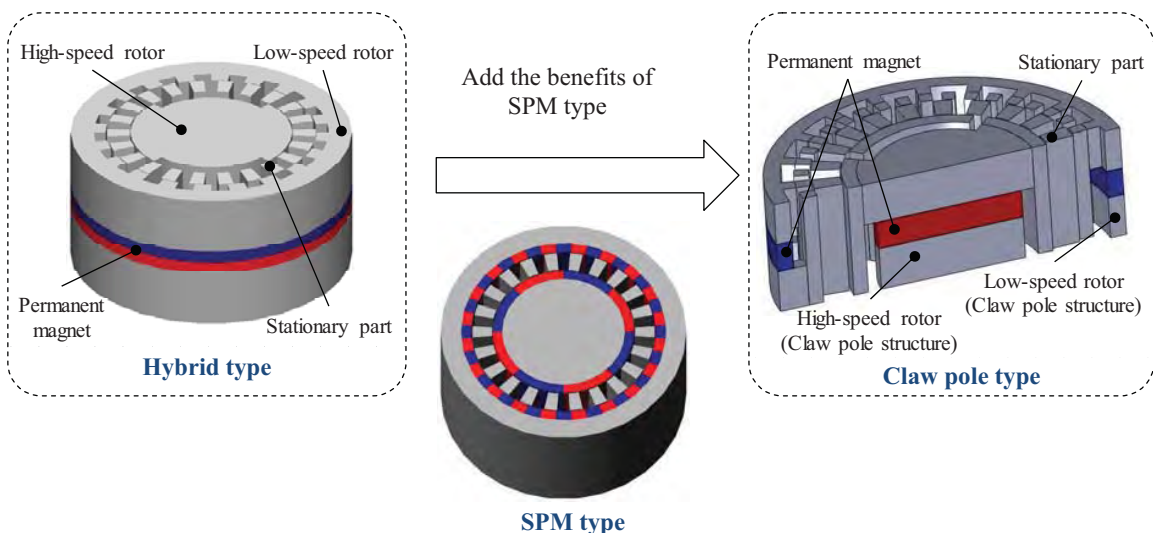


1. Development Background of Magnetic Gears



Position of the SPM-type Magnetic Harmonic Gear at the Hirata Laboratory, Osaka University.

- SPM type are used for the fundamental research of a magnetic gear.
- The knowledge gained from an SPM-type magnetic harmonic gear is expanded to the other magnetic gears.

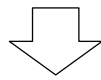
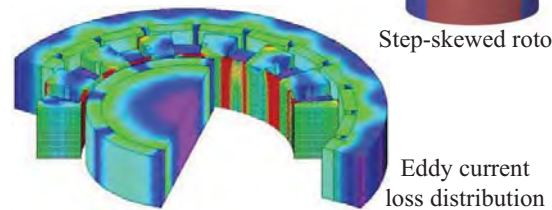
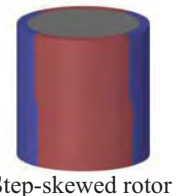
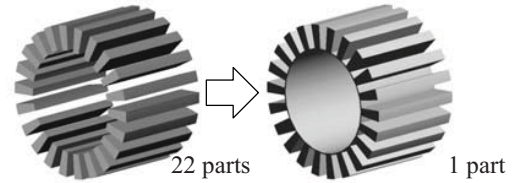


1. Development Background of Magnetic Gears



Development Technology of SPM-Type Magnetic Harmonic Gear

- High productivity
 - The stationary pole pieces are connected with each other by a flux path.
- Low cogging torque
 - Cogging torque is reduced by the step skew of the high speed rotor
- Highly efficient transmission
 - The losses are reduced by using laminated silicon steel sheet.
 - The eddy current loss distribution is clarified.
- Quiet operation (smooth transmission)

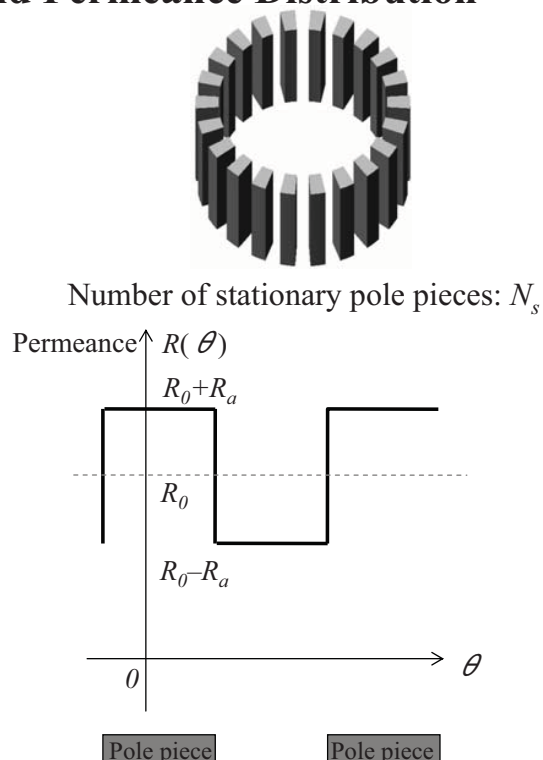
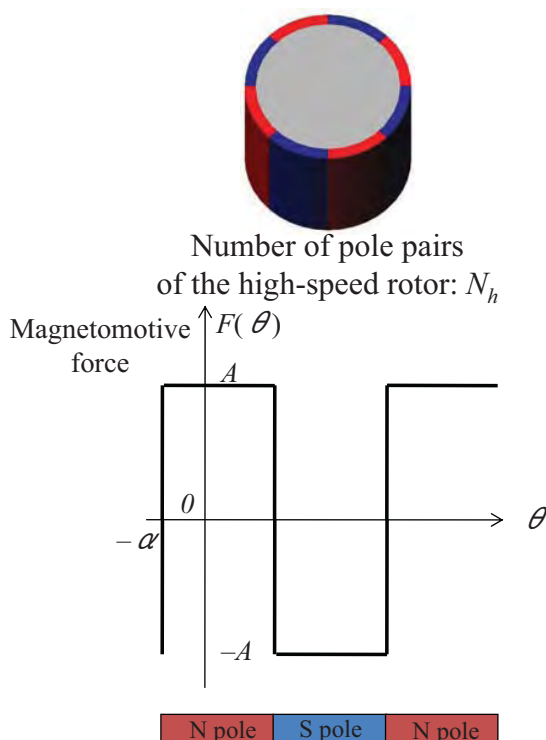


There have been very few reports related to the noise.
Here, the efforts undertaken by the Hirata Laboratory are introduced.

2. Operating Principles of Harmonic Magnetic Gears



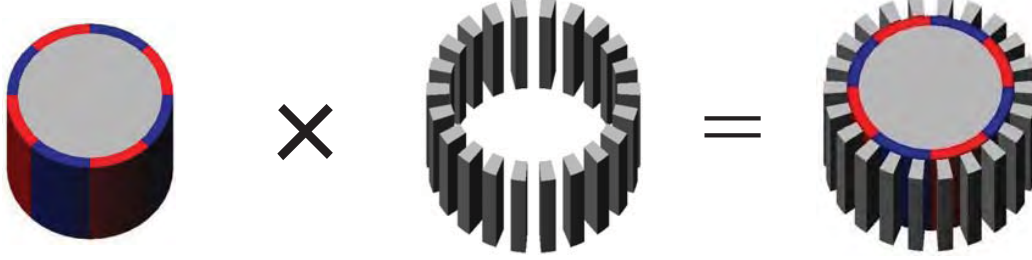
Magnetomotive Force and Permeance Distribution



2. Operating Principles of Harmonic Magnetic Gears



Generation of the Harmonic Magnetic Flux



Magnetomotive force distribution $F(\theta)$ Permeance distribution $R(\theta)$ Magnetic flux distribution $\phi(\theta)$

$$\phi(\theta) = \sum_{m=1}^{\infty} \frac{4AR_0}{(2m-1)\pi} R_0 \sin\{(2m-1)N_h\theta\} + \sum_{l=1}^{\infty} \sum_{m=1}^{\infty} \frac{8AR_a}{(2l-1)(2m-1)\pi^2} [\cos\{(2l-1)N_s - (2m-1)N_h\}\theta - \cos\{(2l-1)N_s + (2m-1)N_h\}\theta]$$

Components contained in the magnetic flux $\phi(\theta)$

$$\begin{cases} H_1(m) = (2m-1)N_h \\ H_2(l, m) = (2l-1)N_s - (2m-1)N_h \\ H_3(l, m) = (2l-1)N_s + (2m-1)N_h \end{cases}$$

l, m : Positive integer

2. Operating Principles of Harmonic Magnetic Gears



Rotation Speed of Harmonic Magnetic Flux

If the high-speed rotor rotates $\Delta\theta$,

$$\phi(\theta) = \sum_{m=1}^{\infty} \frac{4AR_0}{(2m-1)\pi} R_0 \sin\{H_1(m)(\theta + \Delta\theta)\} + \sum_{l=1}^{\infty} \sum_{m=1}^{\infty} \frac{8AR_a}{(2l-1)(2m-1)\pi^2} \left[\cos\left\{H_2(l, m)\left(\theta - \frac{H_1(m)\Delta\theta}{H_2(l, m)}\right)\right\} - \cos\left\{H_3(l, m)\left(\theta + \frac{H_1(m)\Delta\theta}{H_3(l, m)}\right)\right\} \right]$$

$H_1(m)$, $H_2(l, m)$, and $H_3(l, m)$ rotate;

$$H_1(m) : \Delta\theta$$

$$H_2(l, m) : -\frac{H_1(m)\Delta\theta}{H_2(l, m)}$$

$$H_3(l, m) : \frac{H_1(m)\Delta\theta}{H_3(l, m)}$$

The number of pole pairs of the low-speed rotor N_l is selected to synchronize these harmonic magnetic flux.

$$\Rightarrow N_l = \begin{cases} H_2(l, m) \\ H_3(l, m) \end{cases}$$

Synchronizing to $H_1(m)$ gives the magnetic coupling.

2. Operating Principles of Harmonic Magnetic Gears



Formulation of Magnetic Harmonic Gear

Relationships of N_s , N_l , and N_h

$$(2l-1)N_s = N_l \pm (2m-1)N_h$$

(Stationary pole pieces) = (Low-speed rotor pole pairs) \pm (High-speed rotor pole pairs)

Gear ratio

$$G_r = \mp \frac{(2m-1)N_h}{N_l}$$

Transmission torque

$$\omega_h T_h = \omega_l T_l + P_{loss}$$

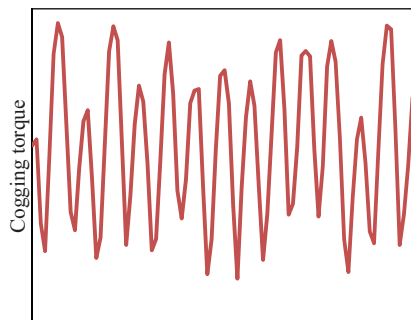
ω_h : Rotation speed of the high-speed rotor; ω_l : Rotation speed of the low-speed rotor; P_{loss} : Loss energy
 T_h : Transmission torque of high-speed rotor; T_l : Transmission torque of low-speed rotor

3. Causes of Vibration



Causes of Vibration in the Low-Speed Rotor

Deformation of the radial component
of the cogging torque



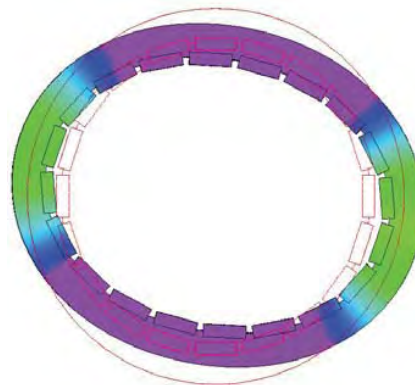
Rotation angle of the low-speed rotor

Specific vibration component
and its harmonic component

+

Vibration components due to the dimension
and assembly errors

Deformation due to the electromagnetic force



Example: 2nd order deformation mode

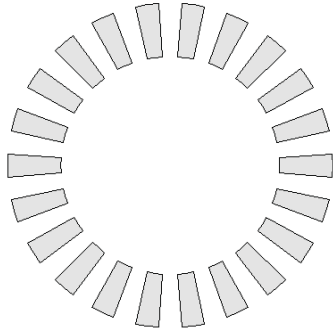
Specific vibration component
and its harmonic component

3.1. Vibrations Caused by Cogging Torque



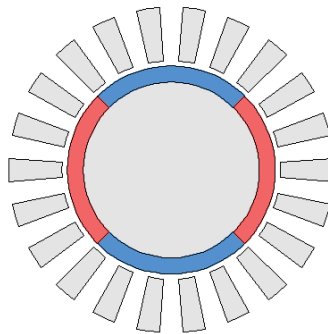
Causes of Cogging Torque in the Low-Speed Rotor

(1) Effects of the stationary pole pieces



Number of stationary pole pieces: N_s

(2) Effects of the harmonic magnetic flux



Harmonic magnetic flux
 $H_1(m) = (2m-1)N_h$
 $H_2(l, m) = (2l-1)N_s - (2m-1)N_h$
 $H_3(l, m) = (2l-1)N_s + (2m-1)N_h$

Imaginary magnet

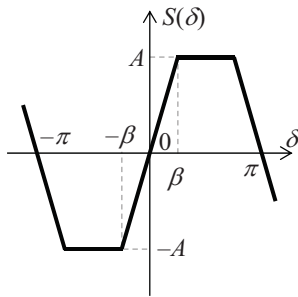
- N_h pole pairs
- $N_s - N_h$ or $N_s + N_h$ pole pairs

An equal number to the low-speed rotor pole pairs doesn't cause cogging torque.

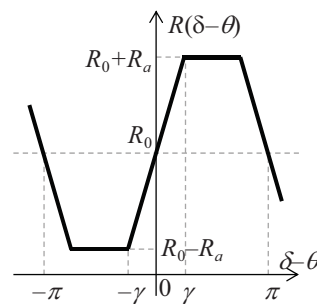
3.1. Vibrations Caused by Cogging Torque



Calculating the Theoretical Cogging Torque Equation



Magnetomotive force distribution of the low-speed rotor



Permeance distribution of the stationary pole pieces

Transformation laws from magnetic energy to mechanical energy

$$T(\theta) = -\frac{\partial W(\theta)}{\partial \theta} \quad W(\theta): \text{Magnetic energy}$$

If the magnetic energy is stored only in the air gap:

$$W(\theta) = \frac{l_{gl}}{8\mu_0 r_{gl} L_s \pi^2} \int_0^{2\pi} S^2(\delta) R^2(\delta - \theta) d\delta$$

l_{gl} : Air-gap length, r_{gl} : Average radius of the air gap,
 L_s : Axial length of the air gap, μ_0 : Permeability in vacuum

3.1. Vibrations Caused by Cogging Torque



Theoretical Equation of Cogging Torque

- Cogging torque due to the stationary pole pieces $T_1(\theta)$

$$T_1(\theta) = -\frac{\partial W(\theta)}{\partial \theta} = -\frac{\partial}{\partial \theta} \left\{ \frac{l_{g1}}{8\mu_0 r_{g1} L_s \pi^2} \int_0^{2\pi} \sum_{m=1}^{\infty} \sum_{n=1}^{\infty} -\frac{a_n b_m}{2} \sin(m N_s \theta) \right\}$$

- Cogging torque due to the N_h pole pairs of the imaginary magnet $T_{21}(\theta)$

$$T_{21}(\theta) = -\frac{\partial W(\theta)}{\partial \theta} = -\frac{\partial}{\partial \theta} \left\{ \frac{l_{g1}}{8\mu_0 r_{g1} L_s \pi^2} \int_0^{2\pi} \sum_{m=1}^{\infty} \sum_{n=1}^{\infty} R_0^2 c_m c_n \cos m(N_h - G_r / N_h) \theta \right\}$$

- Cogging torque due to the $N_s \pm N_h$ pole pairs of the imaginary magnet $T_{22}(\theta)$

$$T_{22}(\theta) = -\frac{\partial W(\theta)}{\partial \theta} = -\frac{\partial}{\partial \theta} \left[\frac{l_{g1}}{8\mu_0 r_{g1} L_s \pi^2} \int_0^{2\pi} \sum_{m=1}^{\infty} \sum_{n=1}^{\infty} R_0^2 d_m d_n \cos 2m N_s \theta \right]$$

R_0 : Permeance between the imaginary magnet and low-speed rotor (constant value)

$a_n, b_m, c_m, c_n, d_m, d_n$: Constants depending on m and n

3.1. Vibrations Caused by Cogging Torque



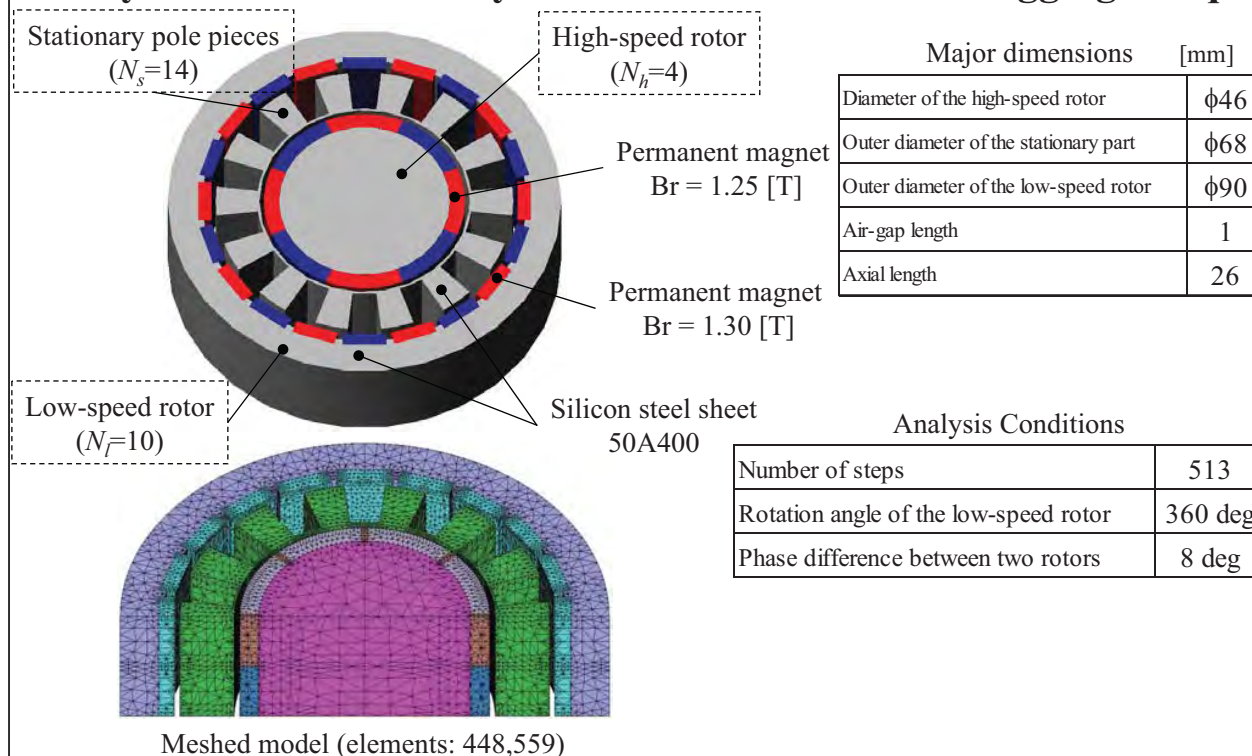
Order of the Cogging Torque

The number of high-speed rotor pole pairs $N_h = 4$, low-speed rotor pole pairs $N_l = 10$, and stationary pole pieces $N_s = 14$ are employed.
Then, the gear ratio $G_r = -0.4$ can be obtained.

Cause	Order
N_s stationary pole pieces	140, 280, 420, ...
N_h pole pairs of the imaginary magnet	140, 280, 420, ...
$N_s + N_h$ pole pairs of the imaginary magnet	140, 280, 420, ...

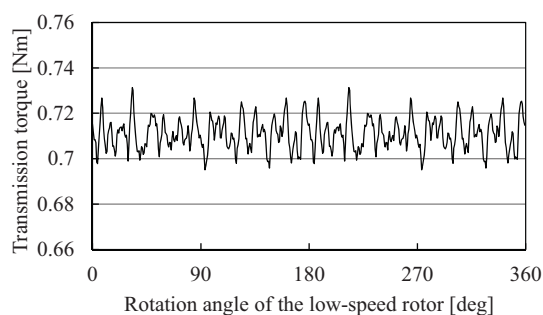
3.1. Vibrations Caused by Cogging Torque

Analysis Model and Analysis Conditions to Obtain Cogging Torque

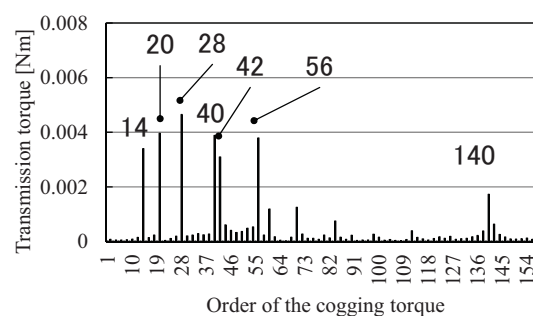


3.1. Vibrations Caused by Cogging Torque

Cogging Torque Analysis Results of the Low-Speed Rotor



Cogging torque waveform



FFT Analysis results

- The cogging torque is 0.03 Nm
- As estimated theoretically, 140th order are detected
- There are harmonic components caused by mesh error in addition to the 140th order components

3.1. Vibrations Caused by Cogging Torque



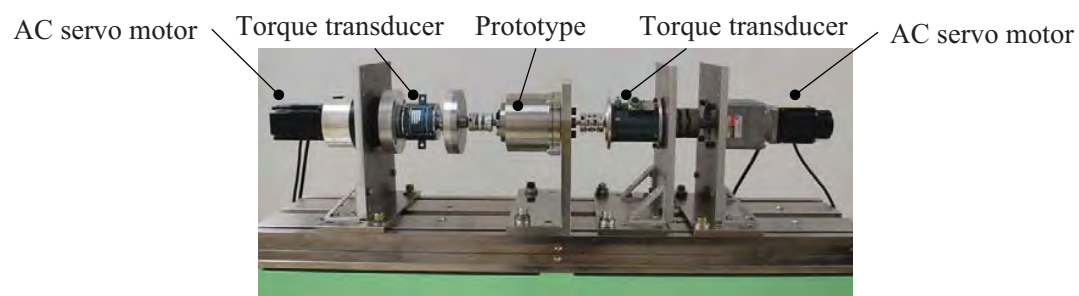
Prototype and Transmission Torque Measuring Equipment



External view of prototype



Internal view of prototype



Evaluation equipment

3.1. Vibrations Caused by Cogging Torque



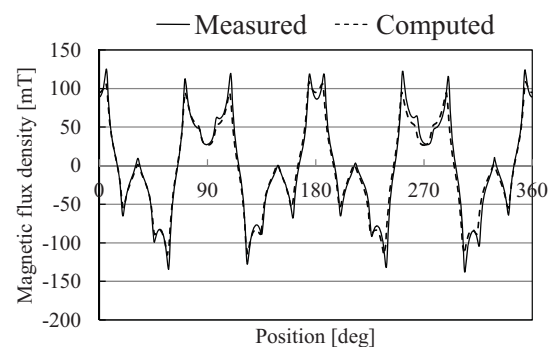
Computed and Measured Harmonic Magnetic Flux



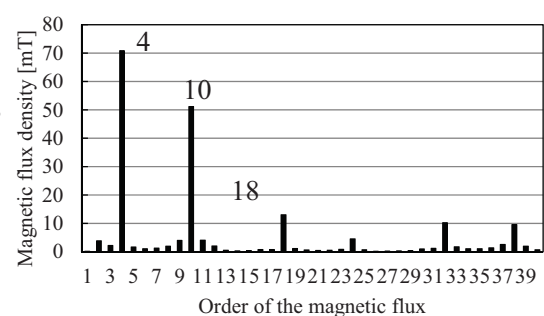
High-speed rotor + stationary part

Measure the magnetic flux density distribution

- The measured and computed results match well.
- The theoretically expected harmonic components are seen.



Magnetic Flux Density Distribution

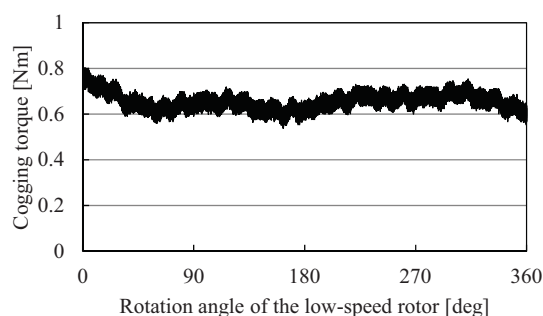


Measured FFT analysis results

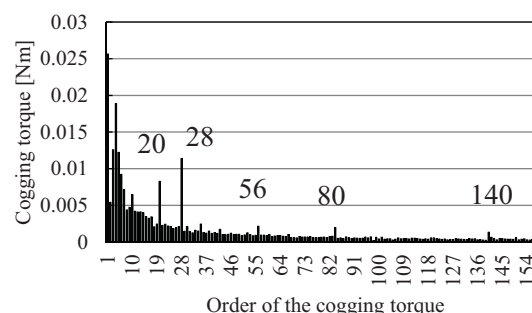
3.1. Vibrations Caused by Cogging Torque



Measured Results of Cogging Torque



Cogging torque waveform



FFT Analysis results

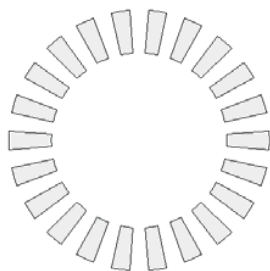
- The cogging torque is 0.22Nm (effects of the servomotor noise))
- 140th order is seen, however the components due to the dimension and assembly errors are dominant.

3.2. Vibrations Caused by Electromagnetic Deformation



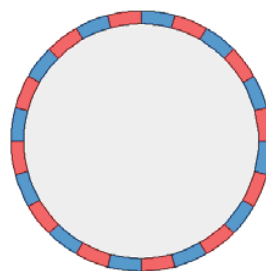
Causes of Electromagnetic Deformation in the Low-Speed Rotor and the Fundamental Deformation Mode

(1) Effects of the stator poles



Stationary pole pieces: 14

(2) Effects of harmonic magnetic flux



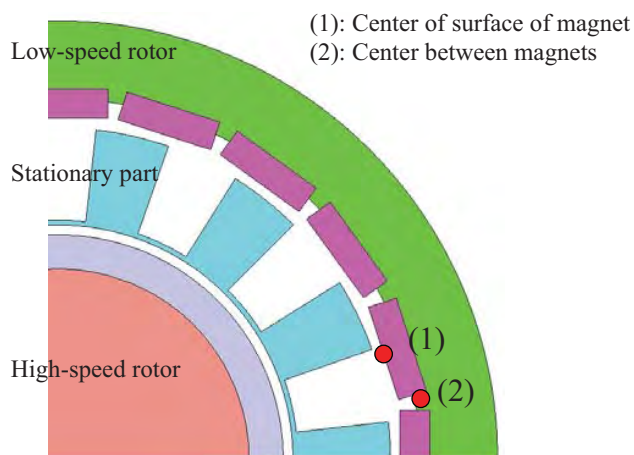
Imaginary magnet
(Fundamental wave of harmonic magnetic flux)

		Rotation speed of magnetic flux distribution	Fundamental deformation mode
Stationary pole pieces	14 pole pieces	0.4 times over the high-speed rotor (Synchronized to the low-speed rotor)	2 nd order
Imaginary magnet	4 pole pairs	Same speed as the high-speed rotor (Synchronized to the high-speed rotor)	2 nd order
	18 pole pairs	0.22 times over the high-speed rotor and same direction	4 th order

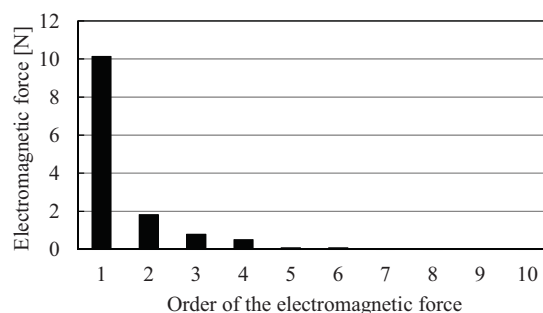
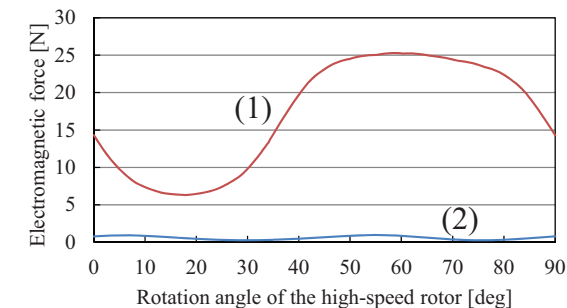
3.2. Vibrations Caused by Electromagnetic Deformation



Period of Electromagnetic Force



The low-speed rotor is fixed and the high-speed rotor rotates 90 deg.
(The stationary part rotates 25.7 deg.)

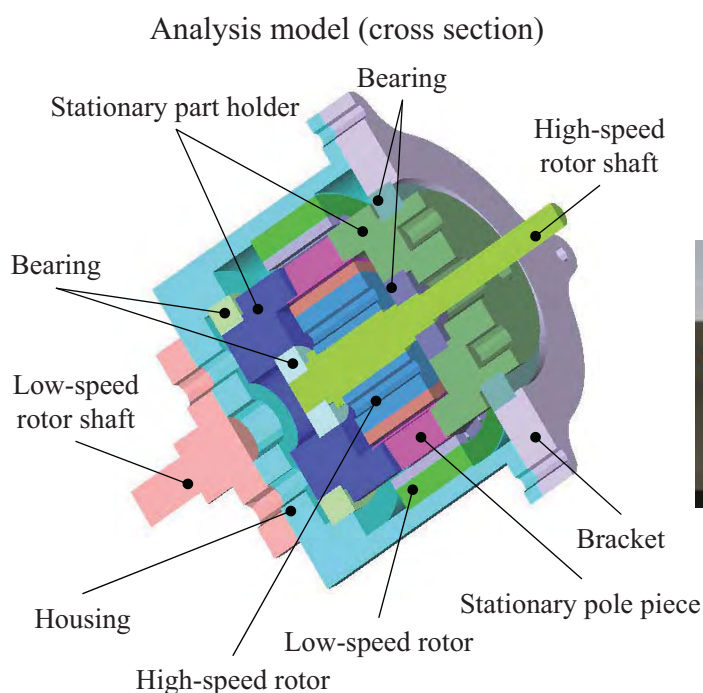


- The effects of the 8-pole imaginary magnet are dominant.
- The period of the electromagnetic force is calculated as 90 deg.

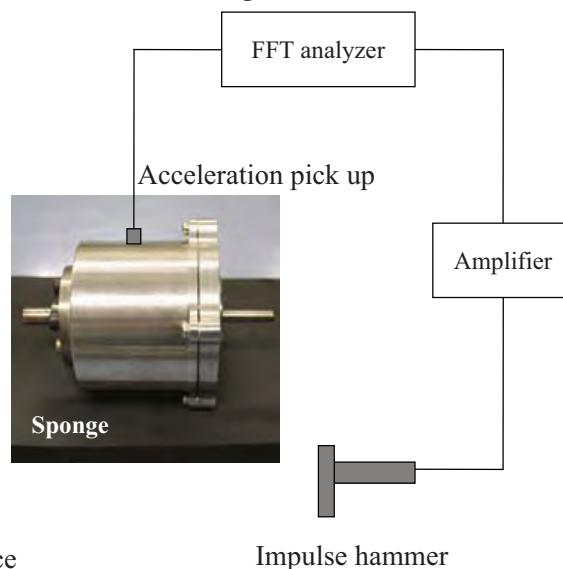
3.2. Vibrations Caused by Electromagnetic Deformation



Analyzing and Measuring the Natural Mode of Vibration



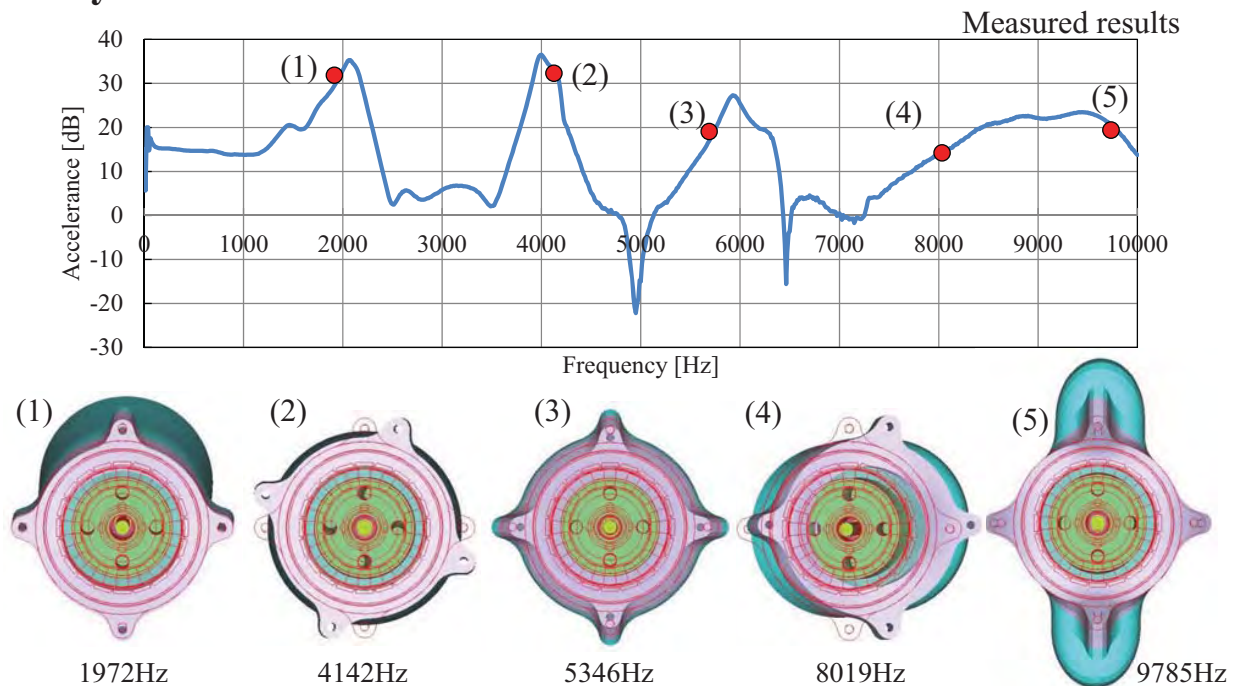
Measuring conditions



3.2. Vibrations Caused by Electromagnetic Deformation



Analysis and Measurement Results of the Natural Vibration Mode

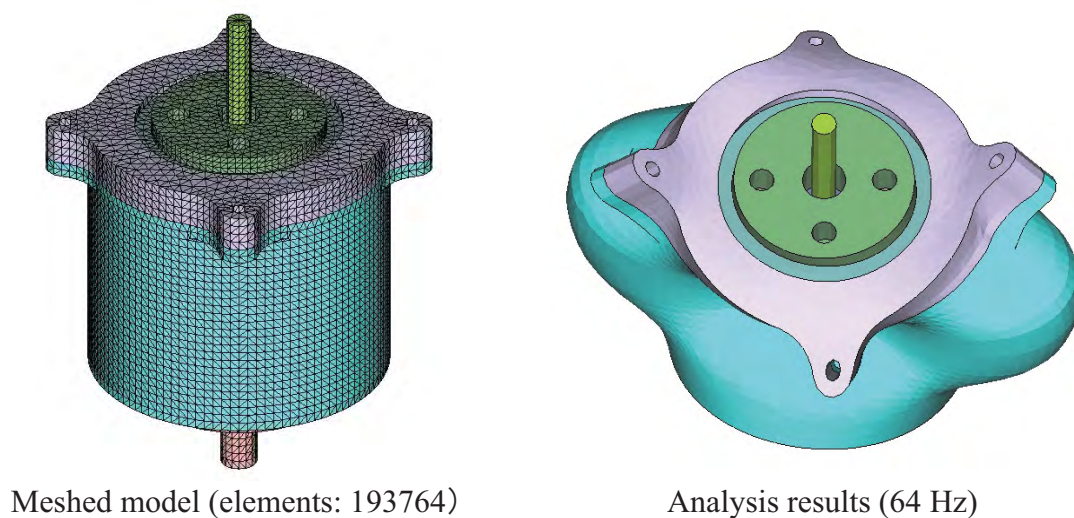


■ Analysis and measurement results match well. ■ 2nd order mode exists nearly at 10 kHz.

3.2. Vibrations Caused by Electromagnetic Deformation



Modal Frequency Response Analysis

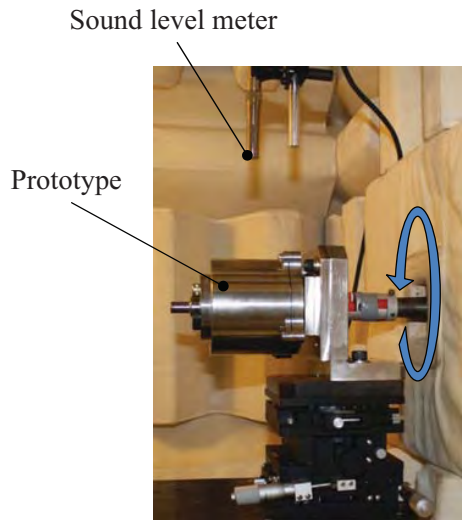


■ 2nd order mode predominates even at non-natural frequency.

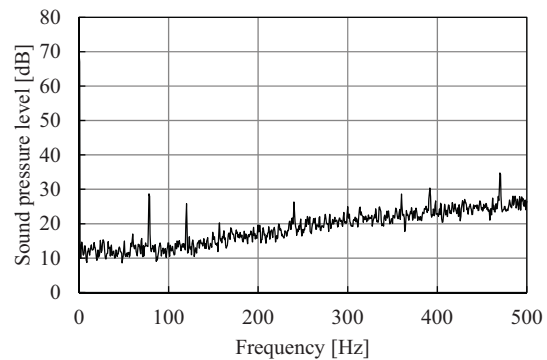
4. Examination by Measuring Noise



Measuring Environment



The high-speed rotor of the prototype in an anechoic chamber is rotated from the exterior by an AC servo motor.



Measured background noise

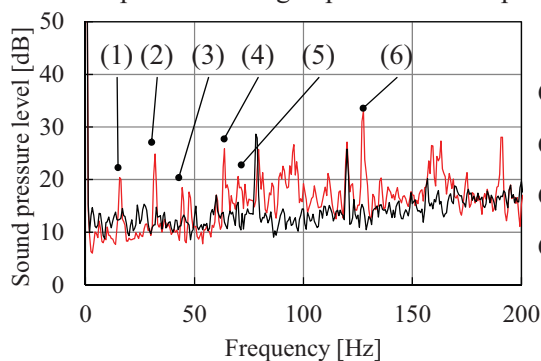
4. Examination by Measuring Noise



Measured Results

Rotation speed of the high-speed rotor: 240 rpm (= 4 Hz)

Rotation speed of the high-speed rotor: 96 rpm (= 1.6 Hz)



■ Noise due to the cogging torque

Cogging torque of the 10th order : $10 \times 1.6\text{Hz} = 16\text{Hz} \dots (1)$

Cogging torque of the 20th order : $20 \times 1.6\text{Hz} = 32\text{Hz} \dots (2)$

Cogging torque of the 28th order : $28 \times 1.6\text{Hz} = 44.8\text{Hz} \dots (3)$

Cogging torque of the 80th order : $80 \times 1.6\text{Hz} = 128\text{Hz} \dots (6)$

■ Noise due to the electromagnetic deformation

2nd deformation mode due to the 4 pole pairs imaginary magnet : $2 \times 6 \times 4\text{Hz} \times 1.4 = 67.2\text{Hz} \dots (5)$

4th deformation mode due to the 18 pole pairs imaginary magnet : $2 \times 18 \times 4\text{Hz} \times 4/18 \times 1.4 = 44.8\text{Hz} \dots (3)$

2nd deformation mode due to the pole pieces : $2 \times 20 \times 1.6\text{Hz} = 64\text{Hz} \dots (4)$

■ Expected orders due to the cogging torque and electromagnetic vibration mode are seen.

5. Conclusion



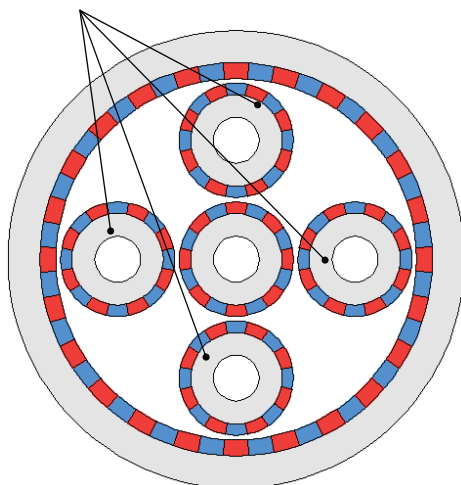
1. The cogging torque of the magnetic harmonic gear was formulated, and the orders were verified by the 3-D finite element analysis and experiment on a prototype.
2. The dominant 2nd order mode of the low-speed rotor was verified by a modal frequency response analysis.
Furthermore, the 2nd order mode does not occur until approximately 10 kHz.
3. The deformation mode of the low-speed rotor was clarified, and the orders due to the cogging torque and electromagnetic vibration were verified by measuring the noise.

Request for JMAG



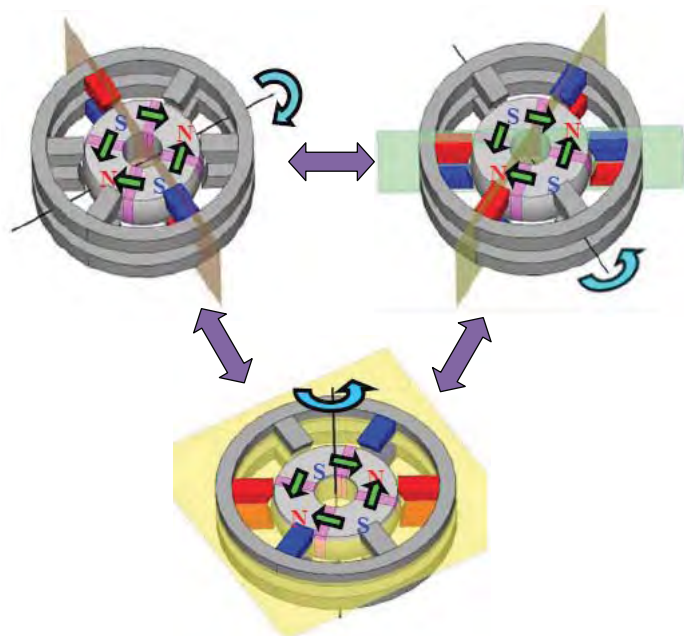
Support for complex motion

Rotational + orbital motion



Magnetic planetary gear

Multi-degree-of-freedom motion





Thank you for your attention.